

Received February 8, 2011; reviewed; accepted April 11, 2011

Gas entrainment rate and flow characterization in downcomer of a Jameson cell

Tuba TASDEMIR, Adem TASDEMIR, Bahri OTEYAKA

Eskişehir Osmangazi University, Dept. of Mining Engineering, Division of Mineral Processing, 26480,
Eskişehir, Turkey, atasdem@ogu.edu.tr, Tel: +90 222 239 37 50 Ext: 3438

Abstract. The Jameson cell which is a new type of gas-liquid contacting device and can be considered as a type of plunging jet column, has been in use worldwide for the separation of fine minerals, coal particles and wastewater treatment etc. Flow characteristics in the downcomer of a Jameson cell are very important since the hydrodynamics of the cell is largely depends on the flow conditions. The hydrodynamics influences flow regimes in the downcomer and hence the gas holdup and bubble diameter are strongly affected by flow conditions. Depending on the air entrainment rate entered to the system, different flow regimes are observed in the downcomer. Bubbly flow which is observed at less air quantities is desired instead of churn-turbulent flow where the gas entrainment rate increase. In this research, the effect of operating conditions including nozzle diameter, downcomer diameter, jet velocity and jet length on gas entrainment rate, Q_g , was evaluated experimentally for an air-water system for the bubbly and churn-turbulent flow. Between these factors, downcomer diameter was found to have very little effect on gas entrainment rate while increasing values of other factors had an increasing effect on it. The results were evaluated by forward stepwise linear regression (MLR) and a piecewise regression with Quasi-Newton estimation of breakpoint (PLR) to estimate the flow conditions and gas entrainment rates. The model by PLR was useful to understand the boundary of the flow characteristics since the two equations were valid in a certain air entrainment ranges, i.e. different flow conditions. The model developed was successful to determine the transition region from bubbly flow to churn-turbulent flow. Experimental data were in good agreement with theoretically predicted value.

keywords: gas entrainment rate, Jameson cell, two phase flow, linear regression

1. Introduction

The solution of the flotation problems is increasingly dependent on more precise understanding of the phenomena involved. The separation selectivity and efficiency of the flotation process depends not only on the differences in the

physicochemical surface properties of various minerals but also on the hydrodynamics of flotation. While there is a substantial and rapidly growing literature on flotation surface chemistry, the deep concern of the hydrodynamics of flotation machines has been neglected to a great extent. As a whole, the flotation process depends on the first hand on surface chemistry controls to provide the potential conditions for particle-bubble attachment and then on the hydrodynamic conditions within the flotation machines which actually develop the attachment between particles and bubbles. In the flotation machines, the hydrodynamic conditions are strongly affected by the air quantity entered to the system. Flotation is an interfacial phenomenon which instead of whose performance depends on the availability of bubble surface area. Thus, airflow rate is an important operational parameter in flotation as it determines the bubble surface area flux.

Bubble columns have been applied successfully as high performance gas-liquid contacting devices in industries such as chemical, biochemical, petrochemical, wastewater treatment and mineral processing. A type of confined plunging liquid jet (CPLJ) bubble column – Jameson cell is used as one of such high performance contactors and is type of a downflow bubble column with gas entrainment by a liquid jet. Jameson Cells are now gaining widespread acceptance for multiphase processes, including mineral and coal flotation and wastewater treatment systems because of its self-sucking characteristics of gas phase and efficient dispersion of the gas phase into liquid phase (Evans et al., 1995, 1996; Jameson and Manlapig, 1991; Mohanty and Honaker, 1999; Jameson, 1999; Yan and Jameson, 2004, Şahbaz et al., 2008).

Since the probability and attachment take place in the downcomer zone of Jameson cell, understanding the hydrodynamic properties of the cell is very important. The hydrodynamic conditions are greatly influenced by the amount of air entering to the downcomer. As the air quantity increases within the downcomer, the turbulent conditions get dominant in the system. This causes particle-bubble detachment for especially coarse particles (Taşdemir et al., 2007a; Çınar et al., 2007). The detachment is a result of action of external forces upon the flotation aggregates which are generated by turbulent motions in the flotation machine and concerns especially large and heavy particles with relatively low hydrophobic properties. The probability of occurrence of this event, apart from the above mentioned factors, depends upon the intensity of turbulence of the medium (Brozek and Mlynarczykowska, 2010).

Many authors studied hydrodynamic properties (gas holdup, gas-liquid interfacial area, mass transfer coefficients etc.) of these contactors (Ohkawa et al., 1985, 1986, 1987; Yamagiwa et al., 1990; Evans, 1990; Evans et al, 2001; Liu and Evans, 1998; Atkinson et al, 2003; Mandal et al, 2003, 2005; Bin, 1993; Evans and Jameson, 1995, Taşdemir et al., 2007b). However, a small number of publications are available regarding gas entrainment rate and flow behavior of CPLJ bubble columns which their hydrodynamics are strongly characterized by different flow patterns depending on the gas flow rate (Ohkawa et al., 1985, 1986, 1987; Yamagiwa et al., 1990; Evans, 1990; Evans and Jameson, 1995). In these studies, the gas entrainment

rate was correlated to a number of variables including nozzle diameter, jet velocity, jet length, column diameter and the flow characteristics in the column were investigated. Okhawa et al. (1985) studied the flow characteristics of downflow bubble columns with gas entrainment by a liquid jet. They observed that there were four types of flow regimes in the column: bubble stagnant flow, non-uniform bubbling flow, uniform bubbling flow and churn-turbulent flow. Yamagiwa et al. (1990) reported that for downflow bubble column, with increasing liquid velocity in the column, flow behavior changed from non-uniform bubbling flow to uniform bubbling flow and then to churn-turbulent flow. But with further increase of liquid velocity, a uniform bubbly flow was again obtained. They also proposed experimental equations for estimating gas holdup and gas entrainment rate. Evans (1990) comprehensively described the performance of confined plunging liquid jet bubble column. From visual observation of flow states in the column, he was found that there were four flow regimes (bubbly flow, slug flow, churn-turbulent flow and annular flow). Evans and Jameson (1995) examined the hydrodynamics of the both bubbly and churn-turbulent flow in the column. Only a few parameters like gas and liquid flow rates, geometry and construction of the nozzle can be controlled by design and operation of these columns. The decisive parameters like gas holdup, gas-liquid interfacial area and mass transfer coefficients are not directly adjustable. Consequently, design and scale-up of CPLJ bubble columns are a difficult task, as the influence of operating conditions, column geometry and physicochemical properties of the phase on the hydrodynamics is not yet fully understood.

In the Jameson Cells, a homogeneous bubbly flow is highly desirable as it offers the maximum gas liquid contacting area with a stable operation. However, in the churn-turbulent regime, the interfacial surface area concentration is considerable lower than in bubbly flow. The transition from bubbly flow to churn-turbulent flow leads to the deterioration of the column performance. Thus, determination the limit of the transition in the downcomer bubble columns is very important. The hydrodynamics of the Jameson cell are strongly characterized by different flow regimes depending on the gas and liquid flow rate. Flow regimes in the column are closely related to gas entrainment characteristics such as gas entrainment rate and gas holdup. However, in the present system of plunging liquid jet where the gas is sucked by high velocity liquid jet, flow regimes and gas entrainment rate primarily depend on properties of free jet such as jet velocity, jet length and nozzle (jet) diameter.

In this research, gas entrainment rate was experimentally measured in a Jameson cell which is a type of plunging liquid jet bubble column by using ranges of nozzle diameters, column diameters, jet velocities and jet lengths. The flow regimes were reported during the experiments and an empirical model predicting gas entrainment was proposed to determine the transition between bubbly flow and churn-turbulent flow in the downcomer for an air-water system by simple measurable variables.

2. Jameson cell and flow regimes in the downcomer

A schematic diagram of a Jameson Cell is shown in Fig. 1. It is comprised of a vertical column (downcomer), which is enclosed at the top and open at the base. The base of the column is below the liquid level in the riser, thus creating an airtight chamber. The liquid feed is in the form of a high velocity jet, which passes through the headspace at the top of the column and entrains gas as it plunges into the liquid inside the column. The plunging jet exchanges momentum with the surrounding fluid which results in a region of high shear, recirculation and energy dissipation, referred to as the mixing zone. The mixing zone forms a turbulent region. In this zone, the entrained gas is broken into fine bubbles. Below the mixing zone is a uniform downward bubbly flow region referred to as the pipe-flow zone. In the pipe flow zone, the turbulence level is significantly lower and the flowing liquid steadily transports bubbles downward. The bubbles then pass into the riser section where they disengage from the liquid (Evans, 1990; Evans et al., 1995).

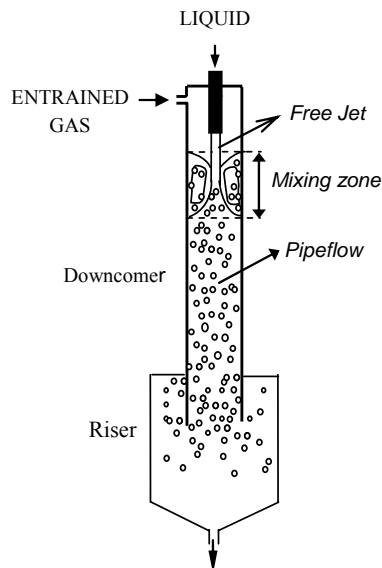


Figure 1. Schematic diagram of a Jameson Cell (Evans et al., 1995)

The flow conditions of bubble column reactors have a significant effect on the operation and performance of bubble column and hence it is desirable to maintain a constant flow regime throughout the column. Depending on the flow conditions there are mainly four types of flow regimes observed in bubble column. They are homogeneous bubbly flow, heterogeneous churn flow, slug flow and annular flow (Mandal et al, 2005; Wild et al, 2003; Evans, 1990; Sanchez-Pino and Moys 1991; Vial et al. 2001; Kantarcı et al, 2005). These are depicted in Fig. 2, where from left to right, superficial gas rate (j_g) in the column is gradually increased. The formation and

stability of these regimes and their limits primarily depend upon parameters like superficial gas velocity, liquid viscosity and velocity.

Bubbly flow occurs at low to moderate liquid and gas flow rate and low void fractions. The gas bubbles have approximately the same size and are homogeneously distributed in the column cross-section. Slug flow occurs with a further increase in gas flow rate. The flow consists of larger, longer, cap-shaped bubbles so called Taylor bubbles. For higher gas flow rate the length and velocity of the slugs increases until the shearing forces present make them unstable. A breakdown of the bubble occurs and the flow is highly turbulent. This type of flow is called churn-turbulent flow. Annular flow occurs at very high gas rate. Annular flow is characterized by liquid flowing as a film around the column wall, surrounding a high velocity gas core.

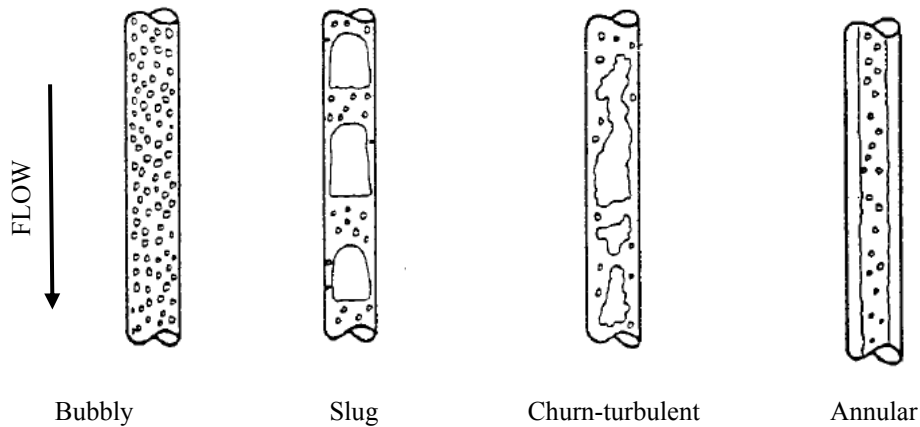


Figure 2. Flow regimes observed in a plunging jet bubble column (Evans, 1990)

For most applications of a Jameson Flotation Cell, the flow regime desired in the pipe-flow zone is bubbly flow. Bubbly flow has advantageous characteristics, most notably its stability and its large interfacial area. As the gas flow rate increases, the flow regimes changes to churn-turbulent flow. Churn-turbulent flow has detriments that include a relatively small interfacial area as well as large bubbles that may coalesce and rise within the column, preventing additional gas flow. From the view point of plunging jet bubble columns, it is therefore pertinent to study the hydrodynamic mechanisms and the flow conditions that transform the flow from bubbly to churn-turbulent (Evans and Jameson, 1995).

3. Materials and method

3.1. Experimental

A schematic diagram of the experimental set-up is shown in Fig. 3. It consists of a feed tank, pump, cell (riser), downcomers in different diameters and nozzles in different diameters which can be mounted simply. The cell which was made of

plexiglass, was 1000 mm high with 195 mm inside diameter. Five downcomer inside diameters were used (16, 21, 26, 36, 46 mm). Each downcomer, made of plexiglass, was 1800 mm length and immersed 400 mm below the liquid surface in the cell. The top of the downcomer housed at different nozzles of 3, 4, 5, 6, 7, 10 mm inside diameter. A centrifugal pump was used to deliver the feed liquid to the nozzle. The liquid flow rate was controlled with a throttling valve in the feed line and a flowmeter was used to measure liquid volumetric flow rate. The manometer was also used to measure the pressure. The air feed into the downcomer was regulated by a valve and volumetric air flow rate was measured using a rotameter. Liquid jet length, distance from the nozzle exit to the liquid surface, were measured by a scale fitted to the downcomer wall.

In the experiments, downcomer diameter (D_C), nozzle diameter (D_N), jet length (L_J) and jet velocity (V_J) were varied within the ranges shown in Table 1. Immersion depth of downcomer and frother quantity were held constant. All experiments were carried out with air-water system at a frother (aerofroth 65, mixture of polyglycols produced by CYTEC Industries) dosage of 20 ppm.. The Jameson cell was operated at several nozzle diameters, downcomer diameters, free jet lengths and jet velocities. To start, these parameters were set to required value. The underflow and overflow from the cell were collected in a feed tank and re-circulated to the downcomer. When the system was at steady state, at each operating parameter, gas entrainment rates were recorded and the flow regimes were determined by visual inspection.

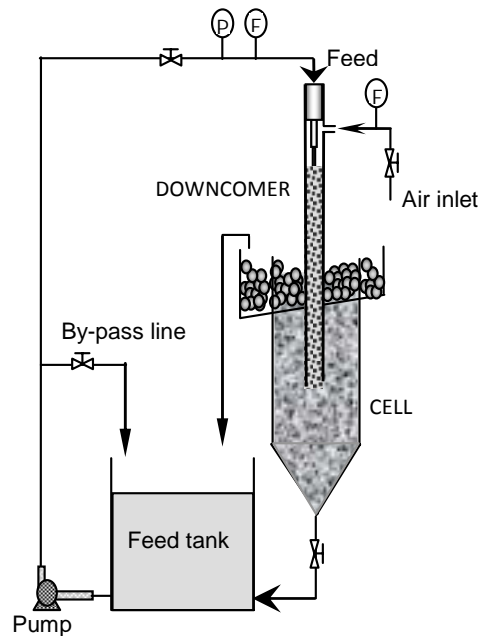


Figure 3. Schematic diagram of experimental apparatus (P: pressure indicator, F: flowmeter)

Table 1. Range of variables in experimental conditions

Downcomer diameter (mm)	: 16, 21, 26, 36, 46
Nozzle diameter (mm)	: 3, 4, 5, 6, 7, 10
Jet length (cm)	: 3, 8, 13, 23, 33, 43
Jet velocity (m/s)	: 6 – 16

3.2. Statistical analyses

After measuring the independent parameters affecting air entrainment rates in Jameson cell, the dependent variable, air entrainment rate, was modeled as a function of independent parameters. Multiple linear regression (MLR) and piecewise linear regression (PLR) were used to obtain quantitative models. These statistical analyses were carried out with STATISTICA 8.0 software package (StatSoft Inc., 1984-2007).

3.2.1. Multiple Linear Regression (MLR)

MLR method provides equation that relates the independent parameters to the air entrainment rate. MLR models usually take the form:

$$Q_g = a_0 + a_1x_1 + \dots + a_nx_n$$

where the intercept (a_0) and the regression coefficients of the predictors (a_i) are determined using least-squares method. The predictors (x_i) included in the equation are used to describe molecular structure of the analysis and n is the number of predictors.

In this study, relationships between the Q_g and the predictors were established by using the forward-stepwise MLR technique.

3.2.2. Piecewise Linear Regression (PLR)

Empirical equation is based on piecewise linear regression method with breakpoint (PLR). Quasi-Newton methods have been used for multi-variant optimization. It is non-linear method that has been used to minimize least square loss function through iterative convergence of predefined empirical equation. The iterative method works for multi-independent variables and dependent variable air entrainment rate both above and below the breakpoint. A non-linear optimization approach achieves acceptable lower residual values with predicted values very close to observed values.

The Quasi-Newton method utilizes the loss function $(observed - predicted)^2$ to arrive at a solution closest possible to observed data. At each iteration loss function is computed to minimize square of difference between the observed and predicted Q_g using pre-defined empirical equation. The method is an optimization process, which runs as long as initial values, stepping values, number of iterations and convergence

criteria are favorable. It terminates if any of these bounding conditions are fulfilled. Therefore, loss function can approach theoretically up to R^2 100%.

In PLR, two separate linear regression equations are produced before and after critical a breakpoint as follows:

$$y = (b_{01} + b_{11}x_1 + \dots + b_{m1}x_m) (y \leq b_n) + (b_{02} + b_{12}x_1 + \dots + b_{m2}x_m) (y > b_n) \quad (1)$$

where b_n is the breakpoint of y values. Each term in parenthesis represents a logical operation. This model estimates two separate linear equations; one for the y values that are less than or equal to the breakpoint (b_n) and one for the y values that are greater than the breakpoint. That model allows the user to specify or estimate breakpoints for the range of the dependent or y values.

4. Results and discussion

4.1. Parameters affecting air entrainment rate in downcomer of Jameson cell

One of the interesting aspects of this type of bubble column is the air entrainment by a liquid jet. Many operating parameters such as jet velocity, jet length, nozzle and downcomer diameters may affect the air entrainment rate. Air entrainment basically occurs due to characteristics of plunging jet and rate of entrainment is mostly controlled by the jet velocity and jet length. The results obtained are presented at various jet velocities in the following plots. Thus, the plots given in here show also the effect of jet velocity on air entrainment rates.

4.1.1. The effect of downcomer diameter

Figure 4 shows the effect of downcomer diameter on the measured air entrainment rate as a function of jet velocity at constant nozzle diameter (3 mm) and jet length (3 cm). The air entrainment rate increases with jet velocity increasing and slightly decreases with downcomer diameter increasing but for D_C up to 36 mm, for higher D_C and jet velocities (10.6 and 12 m/s) air entrainment rate increases what finally gives that influence of D_C can be neglected.

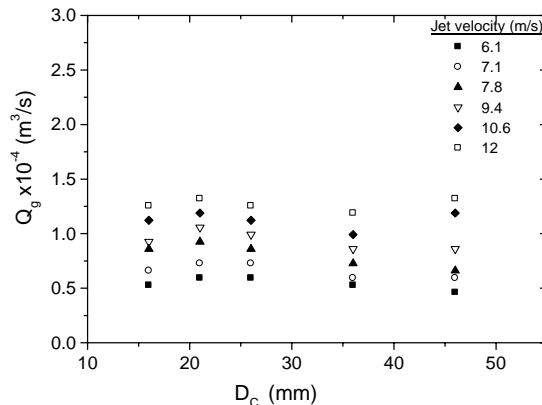


Figure 4. Air entrainment rate versus downcomer diameter for different jet velocities (D_N : 3 mm and L_J : 3 cm)

A generalized plot was given in Figure 5. This figure shows air entrainment rates obtained by different nozzle and downcomer combinations at 3 cm jet length. The plot summarizes air entrainment rate values when different nozzle and downcomer diameters are used. It can be seen that air quantity increases with increasing nozzle diameter at constant downcomer diameter, but almost constant with increasing downcomer diameter. This result is consistent with literature (Yamagiva, et. al., 1990) which was indicating that gas entrainment rate was almost independent of column diameter. Therefore, the diameter of downcomer was held constant and the 36 mm diameter was used in rest of experiments in this study.

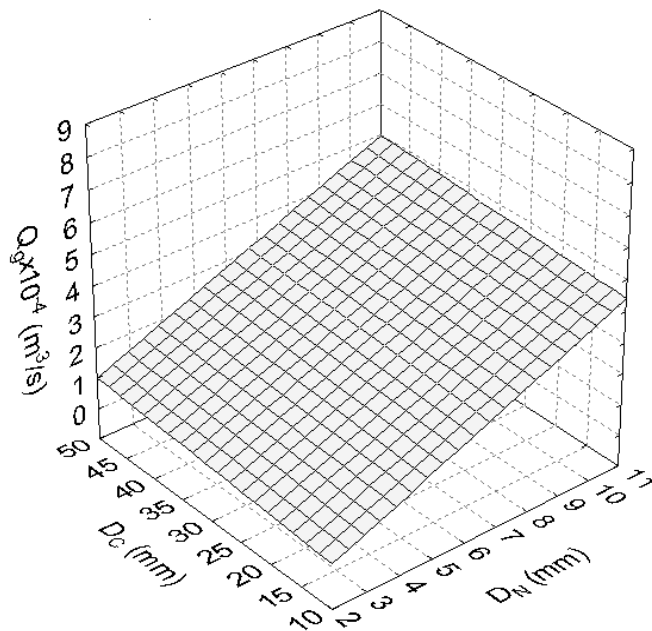


Figure 5. Air entrainment rates obtained with different downcomer and nozzle diameter combinations (L_j : 3 cm)

4.1.2. Effect of nozzle diameter

The effect of nozzle diameter on air entrainment rate is given in Fig. 6. The results obtained at constant downcomer diameter (36 mm) and jet length (3 cm) are shown and plotted as a function of nozzle diameter for each jet velocity tested. It can be seen that for all cases air entrainment rate increased linearly with increasing nozzle diameter at constant jet velocity. It can also be noticed that air entrainment rate increased with increasing jet velocity at constant nozzle diameter. The similar conclusion was reported by Yamagiwa et al., (1990) that air entrainment rate is a function of jet diameter and velocity since energy input into the system increases with their increase.

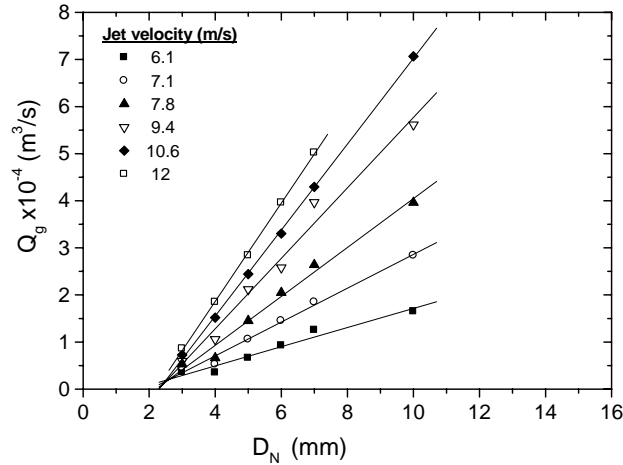


Fig. 6. Air entrainment rate versus nozzle diameter for different jet velocities (D_C : 36 mm and L_J : 3 cm)

4.1.3. Effect of jet length

The relation between the gas entrainment and liquid jet length for various jet velocities measured at constant nozzle and downcomer diameter is presented in Fig. 7. Increasing jet length increases the air quantity entered at constant jet velocities. At constant jet lengths, amount of air entered increases as the jet velocities increases. Jet length is a function of air quantity since increasing amount of air increases the jet lengths.

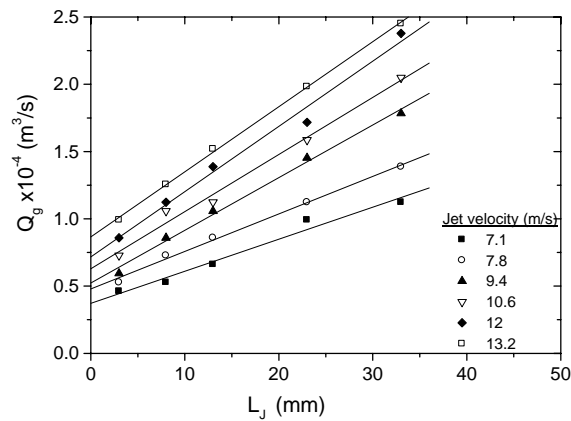


Fig. 7. Air entrainment rate vs jet length for different jet velocities (D_N 3 mm and D_C 36 mm)

In summary, the results indicate that gas entrainment rate was mainly affected by nozzle diameter, jet velocity and jet length parameters. It was also found that the effect of downcomer diameter on it was little compared to other factors and could be negligible. These results are agree with previous studies (Evans, 1990; Evans et al., 1995; Ohkawa et al., 1985, 1987; Yamagiwa et al., 1990; Kusabiraki et al., 1990; Funatsu et al., 1988; Liu and Evans, 1998). The increase in air entrainment rate with increasing with nozzle diameter, jet length and jet velocity was due to the increase in kinetic energy of the jet, surface roughness of the jet and contacting perimeter between the jet and receiving liquid surface. (Evans, 1990; Yamagiwa et al., 1990).

4.2. The flow behavior of gas and liquid in a downcomer of Jameson cell

The flow conditions were reported visually and transition regions from bubbly flow to churn-turbulent flow conditions were determined in each test. The results are given as a function of jet velocity at different jet lengths tested.

In Figure 8, gas entrainment rates have been plotted as a function of jet velocity for each jet length. It can be seen that for all cases the gas entrainment rate increased with increasing jet velocity and jet length. Also from visual observation of flow states in the column, the lines of transition from the bubbly to churn-turbulent flow have been drawn in Fig. 8. These lines define approximate boundaries of these flow regimes. It was observed that flow behavior of the gas-liquid mixture changed from homogenous bubbly flow to churn-turbulent flow with increasing jet velocity and jet length. The similar tendency was also observed in other experimental conditions as the nozzle diameters were varied. At low volumetric gas values (approximately $Q_g < 3 \times 10^{-4} \text{ m}^3/\text{s}$), bubbly flow exists in the pipe flow zone of downcomer. However as Q_g is increased over a certain limit value, the gas bubbles coalesce to form large bubbles and heterogeneous churn-turbulent flow results.

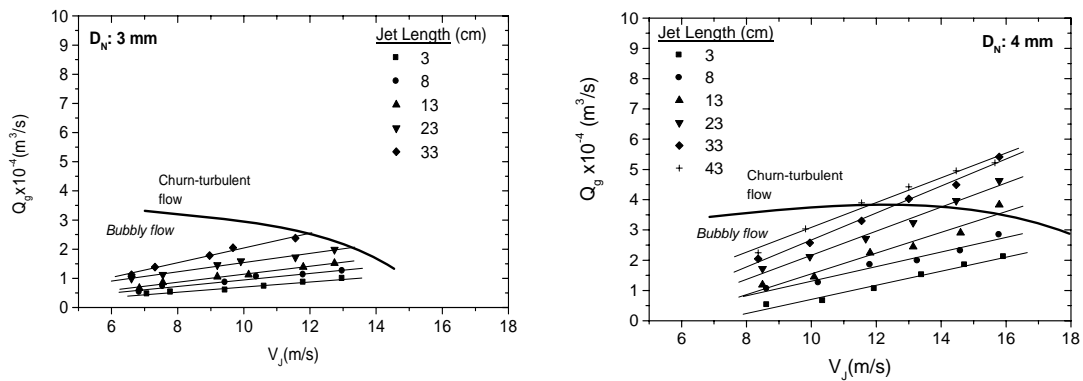
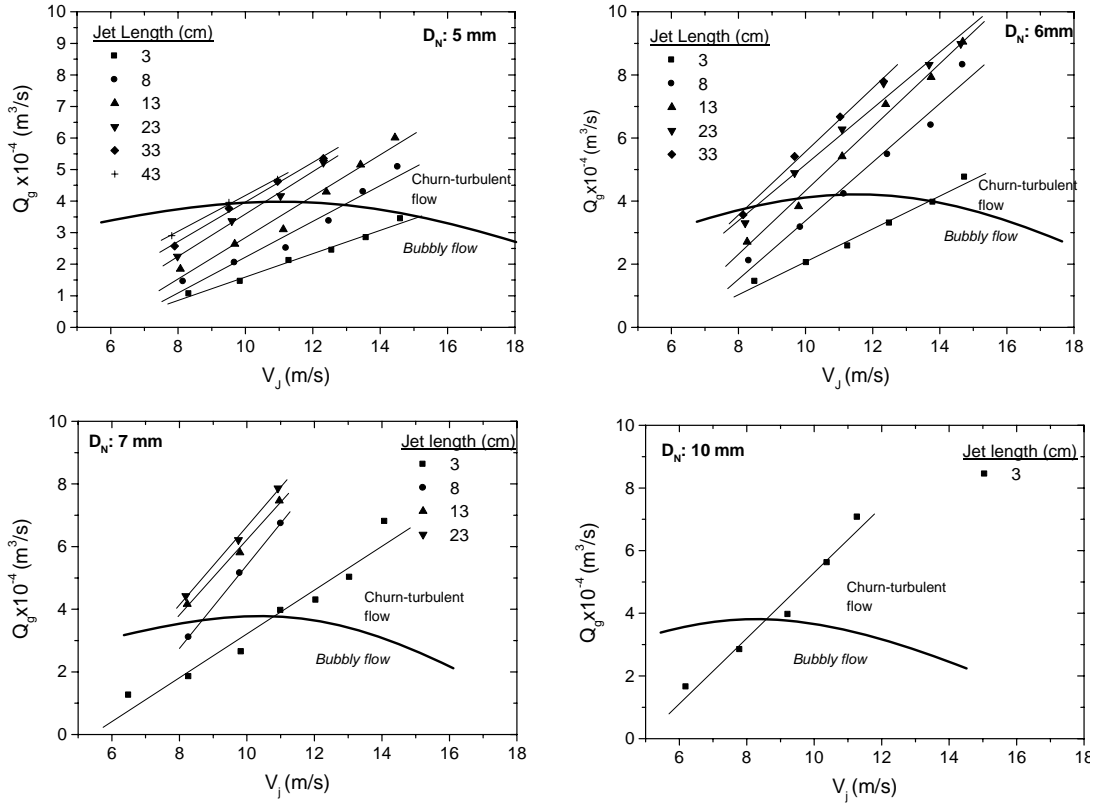


Figure 8. Observed flow regimes and measured air entrainment rates versus jet velocity for different jet lengths (D_C : 36 mm and D_N : 3, 4, 5, 6, 7 mm)



Continuation of Fig. 8.

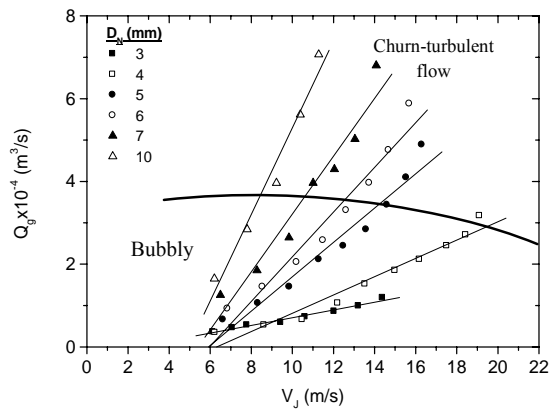


Figure 9. Observed flow regimes and measured air entrainment rates versus jet velocity for different nozzle diameters ($D_C: 36 \text{ mm}$ and $L_J: 3 \text{ cm}$)

The observed flow regimes and effect of nozzle diameter on gas entrainment rate are given in Fig. 9 as a function of jet velocity for a constant downcomer diameter and jet length. It can be seen that the air entrainment rate increased with increasing nozzle diameter at constant jet velocity. The transition from bubbly to churn-turbulent flow is also highlighted in Fig.9. Similar to results presented in Fig. 8, bubbly flows were observed when $Q_g < 3 \times 10^{-4} \text{ m}^3/\text{s}$. When the air entrainment rate exceeds this value, churn-turbulent flow regimes were dominant in the system.

4.3. Statistical analyses for air entrainment rate

Air entrainment rate is considered as dependent variable that varies proportionally with independent variables like nozzle diameter (D_N), jet velocity (V_J) and jet length (L_J).

The results were first evaluated by applying a forward stepwise MLR to identify the most effective variable or variables on the air entrainment rate. In the first step, each of the independent variables are evaluated individually and the variable that has the largest F value greater than or equal to the F to enter value is entered into regression equation. Table 2 summarizes the obtained results. The nozzle diameter, D_N , met the F to enter criteria first and was added to the model firstly, indicating that it is the most effective variable on air entrainment rate compared to other variables. The other important variables in sequences are jet velocity and jet length. All these parameters are statistically significant according to the p values.

Table 2. Estimation of the relationship between Q_g and independent variables by multiple regression stepwise method

	Intercept	Coefficient D_N	Coefficient V_J	Coefficient L_J	R^2	F to enter	p
Step 1	-0.343	0.738			0.31	66.45	0.0000
Step 2	-0.785	0.795	0.371		0.55	88.74	0.0000
Step 3	-6.828	0.918	0.400	0.076	0.73	130.49	0.0000

Table 3. Estimation of the relationship between Q_g and independent variables by PLR method

Intercept ₁	Coef. D_N	Coef. V_J	Coef. L_J	Intercept ₂	Coef. D_N	Coef. V_J	Coef. L_J	Breakpoint	R^2
-2.753	0.425	0.204	0.048	-8.705	1.091	0.523	0.068	3.3×10^{-4}	0.85

However, according to the determination coefficient of the forward stepwise MLR (R^2) it is difficult to model such a dynamic relation using conventional linear methods. Variations of D_N , V_J and L_J do not follow any distinct linear combination and with respect to Q_g . Therefore, a non-linear estimation approach is used to compute the relation between a set of independent variables and a dependent variable. A PLR empirical equation is devised and solved using non-linear Quasi-Newton method. Q_g

estimation equation with coefficients is derived by minimizing loss function for Q_g separately. The analysis results are given in Table 3.

PLR model represents a significant improvement compared to the MLR model. PLR model explains 12% more of the variance ($R^2=0.73$) in the air entrainment rate than MLR model. The PLR model explains more than 85% of the variance of Q_g in the downcomer prediction set versus only 73% explained by the MLR. These improvements can be better seen in Fig. 10 (a) and (b), where observed versus predicted air entrainment rates are plotted for both MLR and PLR approaches respectively. It can be seen that the great dispersion of data points obtained by MLR, especially for prediction set, and the significant improvement reached for the same data sets when the PLR method is employed. Fig. 10 (a) reveals curvature in the plots which an indication that nonlinear relationships exist between Q_g and the predictors in the MLR model.

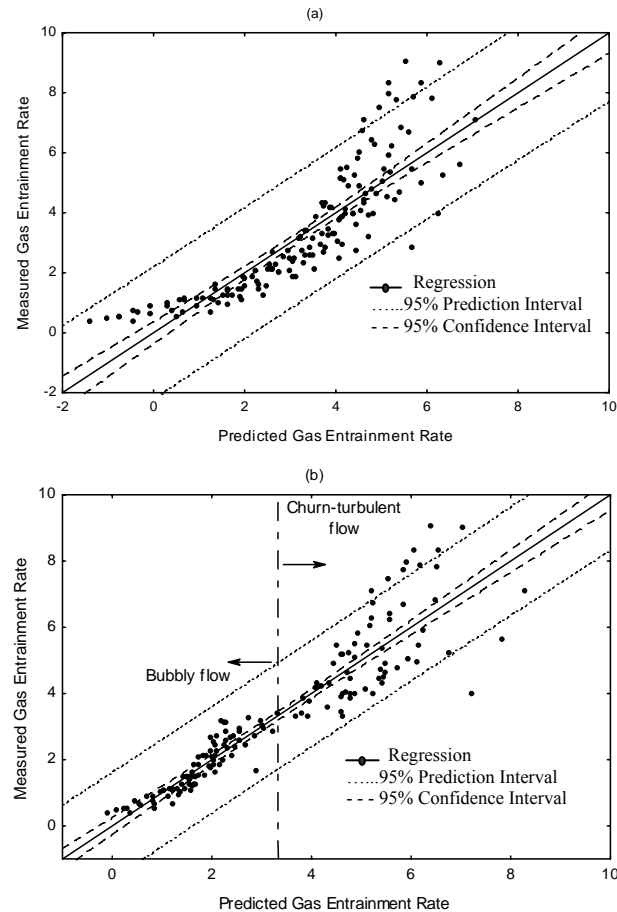


Figure 10. Graphical comparison of predicted versus observed results obtained by MLR model (a) and PLR model (b)

Given that the regression coefficient obtained using PLR model was higher than in MLR model, it seems that there is a discontinuity in the relationship between the dependent and the independent variable, Q_g . In the present case, the breakpoint was $3.3 \times 10^{-4} \text{ m}^3/\text{s}$, which is predicted by the software. This breakpoint determined by the model was coherent with the visual observations during the experimental studies. Thus, model suggests that bubbly flow conditions exists in the system if the gas entrainment rate is equal to or smaller than $3.3 \times 10^{-4} \text{ m}^3/\text{s}$. Otherwise, the churn-turbulent flow occurs when $Q_g > 3.3 \times 10^{-4} \text{ m}^3/\text{s}$. The PLR model showed adequate fits as indicated by its high correlation coefficient ($R = 0.92$) showing a discontinuous relationship between variables.

The agreement between predicted and observed air entrainment rates is clearly better before breakpoint since the predicted values are closer to the regression line as compared to predicted values after breakpoint. The performance of the piecewise linear regression after breakpoint of $3.3 \times 10^{-4} \text{ m}^3/\text{s}$ during the fitting procedure clearly reveals a significant scattering of the computed data points with respect to the ideal trend. This might be due to the fact that the coefficients of D_N , V_J and L_J variables were almost two times higher after breakpoint, (Table 3). This could mean that increasing of these parameters causes the dominant churn-turbulent flow conditions, resulting in undesired flowing in the downcomer.

5. Conclusions

In the present work, gas entrainment rate and flow characteristics of a Jameson cell were experimentally investigated. The effect of nozzle diameter, downcomer diameter, jet velocity and jet length on gas entrainment rate for the bubbly and churn-turbulent flow are determined in two phase gas-liquid system. It was found that the rate of gas entrainment is strongly dependent on these parameters, except downcomer diameter. Gas entrainment rate increased with increasing nozzle diameter, jet velocity, and jet length and was almost independent of downcomer diameter.

It was found that flow regimes in the column were closely related to gas entrainment rate and gas entrainment rate primarily depended on properties of free jet such as jet velocity, jet length and nozzle (jet) diameter. The importance of variables on Q_g was arranged as nozzle diameter, jet velocity and jet length respectively by forward stepwise MLR. From visual observation of flow states in the column, transition boundaries from bubbly flow to churn-turbulent flow conditions were determined. It was shown that flow behavior of the gas-liquid mixture changed from homogenous bubbly flow to churn-turbulent flow with increasing jet velocity, jet length and nozzle diameter due to increased gas entrainment. At low gas volumetric values (approximately $Q_g < 3 \times 10^{-4} \text{ m}^3/\text{s}$), bubbly flow exists in the pipe flow zone of downcomer. However as Q_g exceeds this value, the gas bubbles coalesce to form large bubbles and heterogeneous churn-turbulent flow results.

An empirical model was developed by using piecewise regression with Quasi-Newton estimation of breakpoint to estimate the flow conditions and gas entrainment

rates. The model estimated the breakpoint as $3.3 \times 10^{-4} \text{ m}^3/\text{s}$ which was consistent with the visual observation of flow states in the column during the experiments. The model determined is useful to understand the boundary of the flow characteristics since the two equations was valid in a certain air entrainment ranges, i.e. different flow conditions. The model developed was successful to determine the transition region from bubbly flow to churn-turbulent flow within the ranges of experimental parameters tested in this study.

Acknowledgement

The authors would like to thank Prof. G. J. Jameson for his support and suggestions during design stage of Jameson cell device used in this research.

References

- ATKINSON, B.W., JAMESON, G.J., NGUYEN, A.V. and EVANS, G.M., 2003, Increasing Gas-Liquid Contacting Using a Confined Plunging Liquid Jet, *Journal of Chemical Technology and Biotechnology*, 78: 269-275.
- BIN, A.K., 1993, Gas Entrainment by Plunging Liquid Jets. *Chemical Engineering Science*. 48(21): 3585-3630.
- BROZEK, M. and MLYNARCZYKOWSKA, A., 2010, Probability of Detachment of Particle Determined According to the Stochastic Model of Flotation Kinetics, *Physicochemical Problems of Mineral Processing*, 44: 23-34.
- ÇINAR, M., ŞAHBAZ, O., ÇINAR, F., KELEBEK, Ş. and ÖTEYAKA, B., 2007, Effect of Jameson Cell Operating Variables and Design Characteristics on Quartz Dodecylamine Flotation System, 20: 1391-1396.
- EVANS, G.M., 1990, A Study of a Plunging Jet Bubble Column, Ph. D. Thesis, Newcastle University, Australia.
- EVANS, G.M. and JAMESON G.J., 1995, Hydrodynamics of a Plunging Liquid Jet Bubble Column, *Chemical Engineering Research & Design*, 73: 679-684.
- EVANS, G.M., ATKINSON, B.W. and JAMESON, G.J., 1995, The Jameson Cell, *Flotation Science and Engineering*, Edited by K.A. Matis, 331-363.
- EVANS, G.M., ATKINSON, B.W. and JAMESON, G.J., 1996, Recent Advances in Jameson Cell Technology, *Column'96*, 39-49.
- EVANS, G.M., BIN, A. K., and MACHNIEWSKI, 2001, Performance of Confined Plunging Liquid Jet bubble Column as a Gas-liquid Reactor, *Chemical Engineering Science*, 56: 1151-1157.
- FUNATSU, K., HSU, Y. and KAMOGAWA, T., 1988, Gas Holdup and Gas Entrainment of a Plunging Water Jet with a Constant Entrainment Guide, *Can. J. Chem. Eng.*, 66: 19-28.
- JAMESON, G.J. and MANLAPIG, E.V., 1991, Applications of the Jameson Cell, *Column'91, Proceedings of an International Conference on Column Flotation*, Sudbury, Ontario, 673-687.

- JAMESON, G.J., 1999, Hydrophobicity and Floc Density in Induced-Air Flotation for Water Treatment, *Colloids Surfaces A: Physicochem. Eng. Asp.*, 151: 269-281.
- KANTARCI, N., BORAK, F. and ULGEN, K.O., 2005, Bubble Column Reactors, *Process Biochemistry*, 40: 2263-2283.
- KUSABIRAKI, D., NIKI, H., YAMAGIWA, K. and OHKAWA, A., 1990, Gas Entrainment Rate and Flow Pattern of Vertical Plunging Jets, *Can. J. Chem. Eng.*, 68: 893-901.
- LIU, G. and EVANS, G.M., 1998, Gas Entrainment and Gas Holdup in a Confined plunging Liquid Jet Reactor, *Proceedings of the 26th Australasian Chemical Engineering Conference, (Chemeca 98)*, Port Douglas, Australia.
- MANDAL, A., KUNDU, G. and MUKHERJEE, D., 2003, Gas Holdup and Entrainment Characteristics in a Modified Downflow Bubble Column with Newtonian and Non-Newtonian Liquid, *Chemical Engineering and Processing*, 42: 777-787.
- MANDAL, A., KUNDU, G. and MUKHERJEE, D., 2005, Comparative Study of Two-Phase Gas-Liquid Flow in the Ejector Induced Upflow and Downflow Bubble Column, *International Journal of Chemical Reactor Engineering*, 3: 1-13.
- MOHANTY, M.K. and HONAKER, R.Q., 1999, Performance Optimization of Jameson Flotation Technology for Fine Coal Cleaning, *Minerals Engineering*, 12(4): 367-381.
- OHKAWA, A., SHIOKAWA, Y., SAKAI, N. and IMAI, H., 1985, Flow Characteristics of Downflow Bubble Columns with Gas Entrainment by a Liquid Jet, *J. Chem. Eng. Japan*, 18: 466-469.
- OHKAWA, A., KUSABIRAKI, D., KAWAI, Y. and SAKAI, N., 1986, Some Flow Characteristics of a Vertical Liquid Jet System Having Downcomers, *Chem. Eng. Sci.*, 41: 2347-2361.
- OHKAWA, A., KUSABIRAKI, D., KAWAI, Y. and SAKAI, N., 1987, Flow Characteristics of an Air-entrainment Type Aerator Having a Long Downcomer, *Chem. Eng. Sci.*, 42: 2788-2790.
- SANCHEZ-PINO, S.E. and MOYS, M.H., 1991, Characterization of Co-Current Downwards Flotation Columns, *Column'91*, 1: 341-355.
- ŞAHBAZ, O., ÖTEYAKA, B., KELEBEK, Ş., UÇAR, A. and DEMİR, U., 2008, Separation of Unburned Carbonaceous Matter in Bottom Ash Using Jameson Cell, *Separation and Purification Technology*, 62: 103-109.
- TAŞDEMİR, A., TAŞDEMİR, T., and ÖTEYAKA, B., 2007a, The Effect of Particle Size and Some Operating Parameters in the Separation Tank and the Downcomer on the Jameson Cell Recovery, *Minerals Engineering*, 20: 1331-1336.
- TAŞDEMİR, T., ÖTEYAKA, B. and TAŞDEMİR, A., 2007b, Air Entrainment Rate and Holdup in the Jameson Cell, *Minerals Engineering*, 20/8: 761-765.
- STATISTICA 8.0, StatSoft Inc., 1984-2007.

- VIAL C., PONCIN, S., WILD, G. and MIDOUX, N., 2001, A Simple Method for Regime Identification and Flow Characterization in Bubble Columns and Airlift Reactors, *Chemical Engineering and Processing*, 40: 135-151.
- WILD, G., PONCIN, S., LI, H. and OLMOS, E., 2003, Some Aspects of the Hydrodynamics of Bubble columns, *International Journal of Chemical Reactor Engineering*, 1: 1-36.
- YAMAGIWA, K., KUSABIRAKI, D. and OHKAWA, A., 1990, Gas Holdup and Gas Entrainment Rate in Downflow Bubble Column with Gas Entrainment by a Liquid Jet Operating at High Liquid Throughput, *J. Chem. Eng. Japan*, 23: 343-348.
- YAN, Y.D. and JAMESON, G.J., 2004, Application of the Jameson Cell Technology for Algae and Phosphorus Removal from Maturation Ponds, *Int. J. Miner. Process.*, 73: pp 23-28.